



AERODYNAMIC NOISE RADIATED BY THE INTERCOACH SPACING AND THE BOGIE OF A HIGH-SPEED TRAIN

N. FRÉMION AND N. VINCENT

Vibratec, 28 chemin du Petit Bois B.P. 36, 69131 Ecully Cedex, France

M. JACOB, G. ROBERT AND A. LOUISOT

Ecole Centrale De Lyon, 36 avenue Guy de Collongue, 69131 Ecully Cedex, France

AND

S. GUERRAND

SNCF Direction de la Recherche, 45 rue de Londres, 75379 Paris Cedex 08, France

(Received in final form 23 September 1999)

Full-scale acoustic experiments on a TGV are performed with on-board measurement techniques. Some spectral characteristics of the intercoach spacing and the bogie region are highlighted and interpreted. Two measurement techniques are described; they both extract the acoustical information of a particular aerodynamic source from the signal given by a flow imbedded probe.

© 2000 Academic Press

1. INTRODUCTION

As the speed of modern high-speed trains increases, the trains are not only louder, but rolling noise tends to be dominated by aerodynamic noise in the low-frequency range. Therefore it is important to determine aerodynamic sources when the speed exceeds 250 km/h.

The experimental characterization of the acoustic sources on high-speed vehicles is a difficult task. These sources are usually random noise sources and the study of these sources thus needs an appropriate statistical treatment. The computation of statistical averages requires a minimum number of samples (time series). These samples have to be long enough to contain the main information of the original signal. Therefore the experimental approach determines the possible statistical treatments.

Two approaches are used: The first approach consists of placing a microphone or an antenna on the ground to measure the noise level when the vehicle is passing. With appropriate treatments, the main source locations and levels can be identified. The advantage of this approach is that the signals are acoustic signals. Its drawback

is that the signals have a short duration; this makes it difficult or even impossible to identify correctly the different sources, to describe them statistically, to determine their spectrum or directivity.

The second approach is to attach a microphone-type probe to the vehicle (which will be referred to as “in-flow” probe), to record a stationary (in the statistical sense) signal with this probe and to analyze this signal in order to extract its acoustic part. The advantage of this approach is the availability of long time series and thus the statistical averages. Its main disadvantage is that the measured signal is not purely acoustic; it has an acoustic component which is due to the different noise sources and an aerodynamic component which is due to the fluctuating part of the velocity field (turbulence).

In this study, the second approach is used to characterize the acoustic radiation of the intercoach spacing (ICS) and of the bogie region on a TGV. In the first part, two extraction methods are presented: one is a measurement technique based on the coherent output power spectrum, whilst the other is based on a direct estimate of the noise-to-signal ratio associated with the in-flow probe.

In the next two sections, a full-scale experiment on an ICS and in one bogie region of a TGV is presented. The extraction methods are applied, results are discussed and typical spectra are presented.

2. MEASUREMENT AND PROCESSING METHOD

2.1. OBJECTIVE

Since the objective of the present study is to extract the contribution of a particular source to a noise-polluted signal, it can be represented by a linear single input–single-output problem sketched in Figure 1. The input $u(t)$ features the source and is assumed to be stationary in the statistical sense. The output $v(t)$ is the signal to be characterized (by its spectrum $G_{vv}(f)$). Unfortunately, neither $u(t)$ nor $v(t)$ can be measured directly: only noise-polluted signals $x(t) = u(t) + n(t)$ and $y(t) = v(t) + m(t)$ are accessible. $n(t)$ is the ambient noise of $u(t)$ and $m(t)$ the ambient noise of $v(t)$. $n(t)$ and $m(t)$ are assumed to be uncorrelated. In this paper, G_{vv} is estimated by two methods.

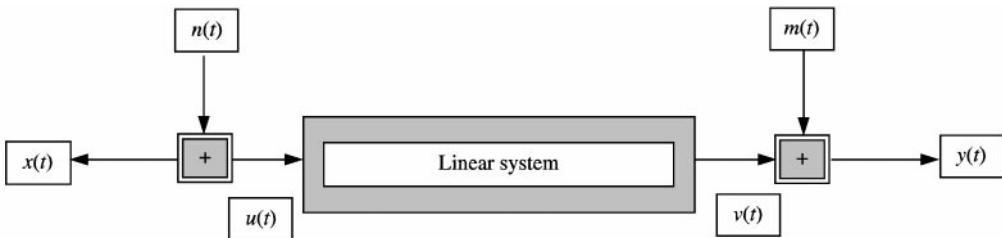


Figure 1. Linear single input–single-output problem.

2.2. THE COP METHOD

The coherent output power (COP) spectrum measurement technique is not new [1]. For the single-input–single-output problem, the COP is defined as the product of the measured output spectrum (G_{yy}) and the coherence $\gamma_{xy}^2(f)$ between the detection signal $x(t)$ and the measured output signal $y(t)$:

$$COP_{xy}(f) = \gamma_{xy}^2(f) G_{yy}(f). \quad (1)$$

It can be shown [1] that the COP is related to G_{vv} by

$$COP_{xy}(f) = \frac{G_{vv}(f)}{1 + NS_x(f)}, \quad (2)$$

where $NS_x(f) = G_{nn}(f)/G_{uu}(f)$ is the noise-to-signal ratio of the detection signal $x(t)$.

Thus, the COP is an estimate of the spectrum G_{vv} . Two main errors are associated with this estimate.

The first is the statistical error due to the fact that the signals are random and that the averages are computed from a finite number of samples (time series). In practise, it can be made arbitrarily small by increasing the number of samples. The second is a bias error due to $NS_x(f)$ as shown by equation (2). If NS_x is small, COP_{xy} is a good estimate of G_{vv} , otherwise it has to be estimated. Since the noise is not correlated to the signal, the noise-to-signal ratio is related to the coherence: for two noisy signals x_1 and x_2 , one has the following relation:

$$\gamma_{12}^2(f) = \frac{1}{[1 + NS_1(f)][1 + NS_2(f)]}. \quad (3)$$

In order to obtain the noise-to-signal ratios of a particular signal (the source signal $u(t)$ in this case), three detection signals x_i are needed. As shown in reference [2], the three noise-to-signal ratios NS_i can then be obtained from equation (3):

$$\begin{aligned} NS_1 &= \frac{\gamma_{23} - \gamma_{12}\gamma_{13}}{\gamma_{12}\gamma_{13}}, \\ NS_2 &= \frac{\gamma_{13} - \gamma_{21}\gamma_{23}}{\gamma_{21}\gamma_{23}}, \\ NS_3 &= \frac{\gamma_{21} - \gamma_{31}\gamma_{32}}{\gamma_{31}\gamma_{32}}. \end{aligned} \quad (4)$$

Therefore, an unbiased estimate of G_{vv} requires three detection signals of the same source $u(t)$ with independent ambient noise ($n_i(t)$).

2.3. DIRECT METHODS

The direct method relies on the fact that the measured output signal $y(t)$ is an estimate of the output signal $v(t)$. This estimate is biased by the noise-to-signal ratio. The spectra are related by:

$$G_{vv}(f) = \frac{G_{yy}(f)}{1 + NS_y(f)} \quad (5)$$

where $NS_y = G_{mm}/G_{vv}$.

Thus, the noise-to-signal ratio NS_y has to be determined. Therefore, the same approach as that used in section 2.2 can be applied. In this case, the three signals can be chosen in the following way:

- two detection signals $x_1(t)$ and $x_2(t)$ which characterize the same source $u(t)$,
- the measured output signal $y(t)$.

2.4. APPLICATION TO THE IN-FLOW DETECTION OF ACOUSTIC SOURCES

In-flow acoustic measurements are quite well featured by the previous model problem. Indeed, the linear system represents the fluid in which the waves are propagating. The input $u(t)$ corresponds to the acoustic source. The detection signal $x(t)$ is a signal which is meant to characterize in some way the investigated source. $n(t)$ is the noise associated with this measurement. Microphones located near the supposed aerodynamic sources are used as detection sensors.

The in-flow acoustic probe measures the signal $y(t)$ which contains the acoustic signal $v(t)$ radiated by the source at the observation point and the noise $m(t)$. $m(t)$ is due to the aerodynamic pressure fluctuations around the probe and the acoustic pressure from sources other than the one under investigation.

To minimize the contribution of the aerodynamic pressure fluctuations to $y(t)$, a microphone with a special turbulence screen (as described by Neise [3]) is used.

For the COP method, three detection sensors are placed in the vicinity of a supposed source location, whereas for the direct method, only two detection sensors are required.

In both cases, the spectra of all the detection and in-flow probes are measured. Moreover, the coherence functions between all these probes can also be measured.

3. RESPONSE TO THE FLOW AND RADIATION OF THE ICS

3.1. EXPERIMENTAL APPROACH AND INSTRUMENTATION

Thirteen sensors are distributed in the ICS (see Figure 2). Their spectra and coherence functions are analyzed to capture the main phenomena induced by the flow and to study their frequency distribution.

The sensor distribution can be divided into four areas:

1. *the cavity* characterized by the sensors P1, P2, P3, P4 and P5,
2. *the left part*, located at the left of the damper, characterized by the sensors P3, P13, P12 and P14,
3. *the right part*, located at the right of the damper, characterized by the sensors P4, P6 and P7,
4. *the junction area between the ICS and the bogie*, characterized by the sensors P8, P18, P9 and P14.

In order to determine whether the phenomena detected on the sensors radiate any sound or not, three Noise probes were mounted downstream of the ICS: N1, N2 and N3 (see Figures 2 and 3); they are distributed along the whole height of the cavity.

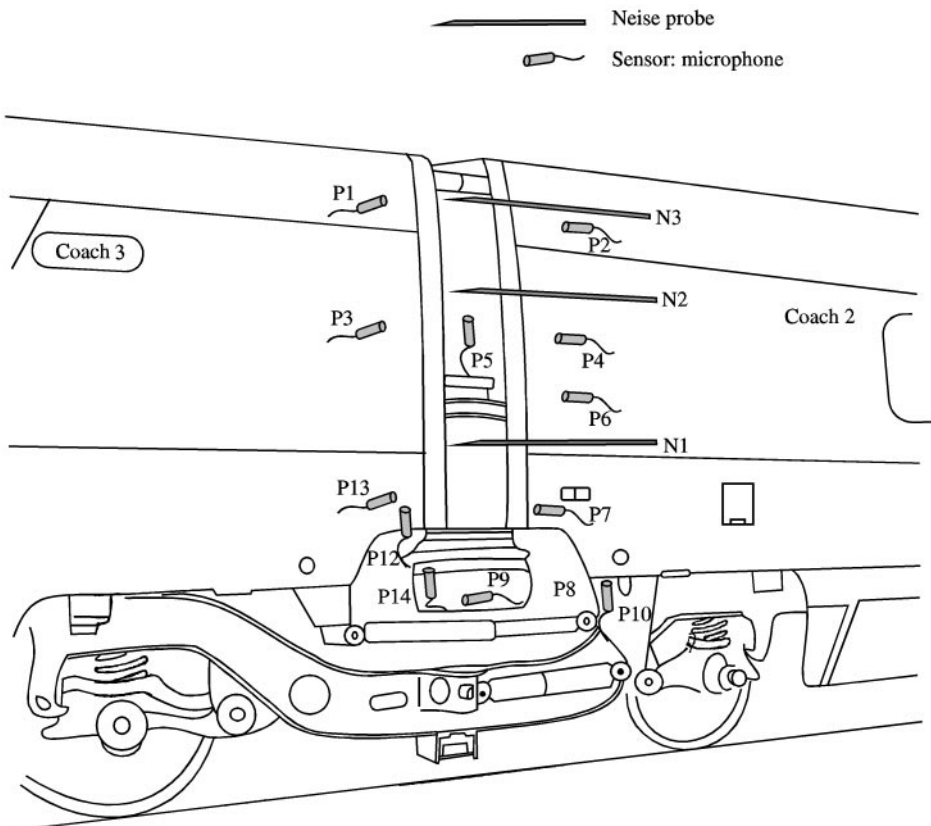


Figure 2. Location of the Noise probes.

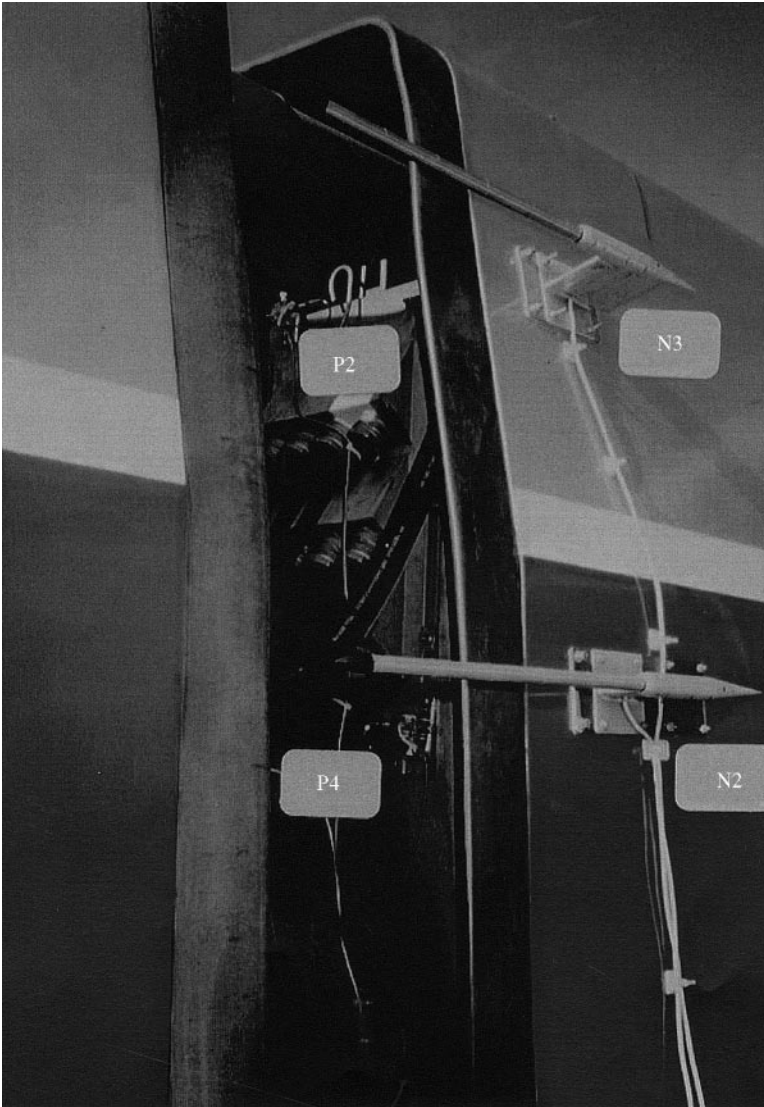


Figure 3. Location picture.

3.2. RESULTS AND ANALYSIS

3.2.1. *Characteristic frequencies*

In order to capture the phenomena induced by the flow in the ICS and to study their frequency distribution, the coherence functions between the sensors located in a same area of the cavity were plotted. The coherence levels are quite high, mainly in areas 1 and 2.

Since it is difficult to list all the frequency peaks of the coherence functions, the most significant sensors in each cavity area are selected and an average of their coherence functions is computed (see Figure 4). The main frequencies detected on

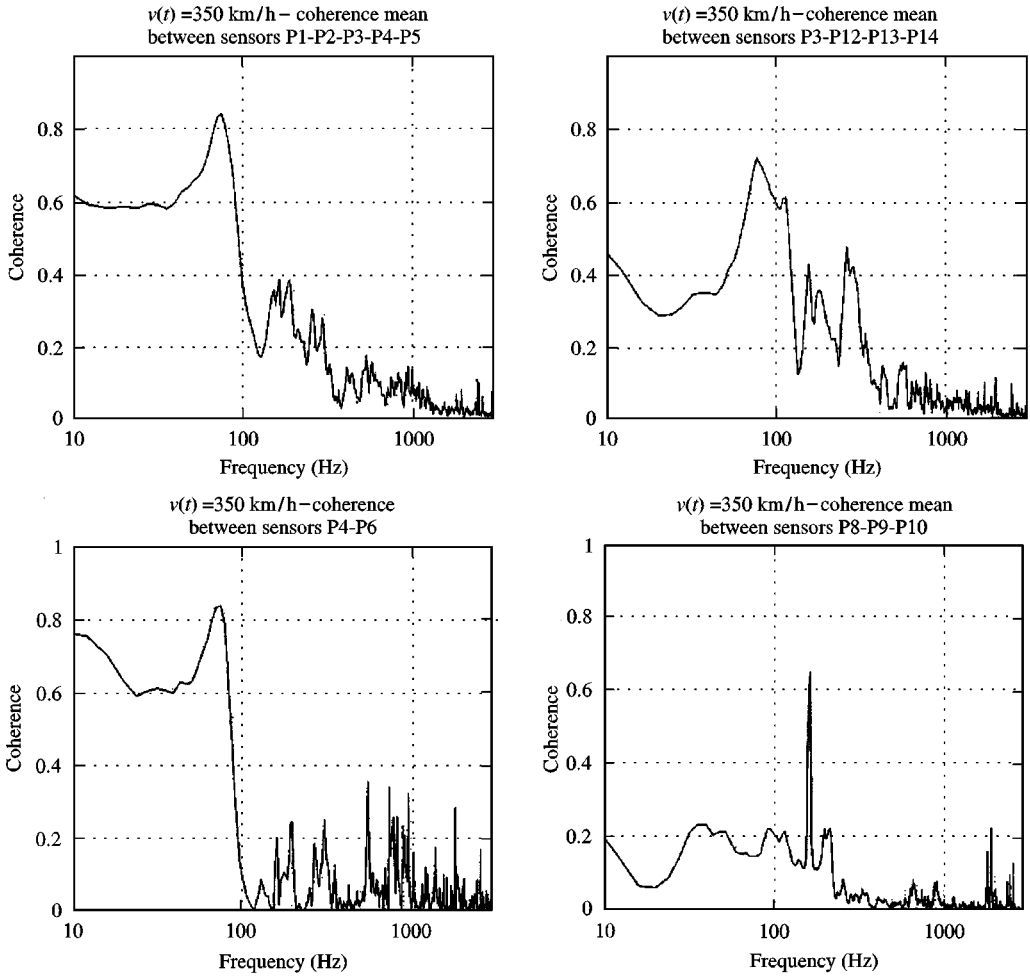


Figure 4. Average coherence functions of each area of the ICS.

these average curves are listed. Peaks at some of these frequencies are also apparent in the corrected spectra obtained with the COP technique on the three Noise probes (see Figure 5): 76, 108, 164, 196, 212 and 276 Hz. Their levels vary from one Noise probe to another; some are not detected on each probe. Furthermore, the origin of each peak can be associated with either the global phenomenon of the whole cavity or with a local phenomenon occurring in a particular region of the cavity.

For the main peaks, the following indications on the radiating regions and their radiation directivity are obtained:

- 76 Hz: comes from the whole cavity and radiates in all directions,
- 108 Hz: is a typical phenomenon of the upper part of the cavity which has a pronounced directivity,

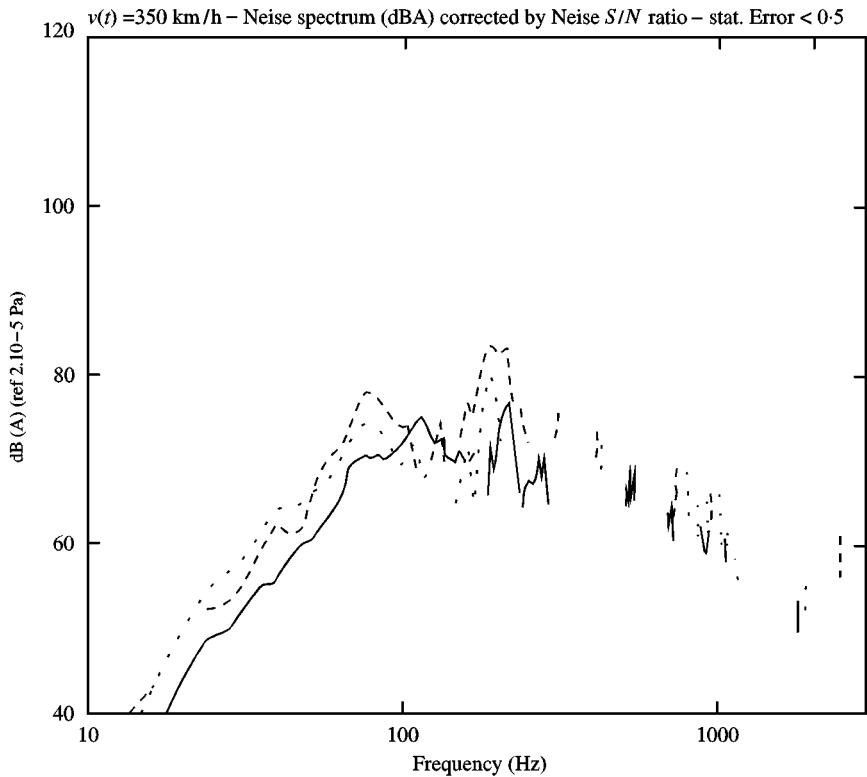


Figure 5. Comparison between the three global noise spectra, associated with the radiation of the whole cavity and obtained with the three Neise probes N1, N2 and N3. —, Neise N3: 96.69 dB (A); ----, Neise N2: 103.2 dB (A); ····, Neise N1: 99.12 dB (A).

- 164 Hz: the sleeper-passing frequency is only detected in the lower part of the cavity on Neise probe N1,
- 196 Hz: is detected in the whole cavity and it radiates outwards along the entire height of the cavity,
- 212 Hz: has its source in the lower part of the cavity but radiates mainly in the middle, on Neise probe N2,
- 276 Hz: radiates in the upper part of the ICS but its origin is the central part of the cavity.

Some of the radiating frequencies can be correlated to the cavity modes computed numerically with a 2-D infinite finite element (IFEM) model and measured in the upper part of the space between the coaches under artificial acoustic excitation. More precisely, the peak at 76 Hz probably corresponds to the first vertical mode, the peak at 196 Hz to the first section mode in the depth of the cavity and the peak at 276 Hz to the second mode in the width of the cavity (see Figure 6). Thus, the study of the cavity acoustic response explains the mechanism which generates the most relevant peaks of the sound radiated by the ICS.

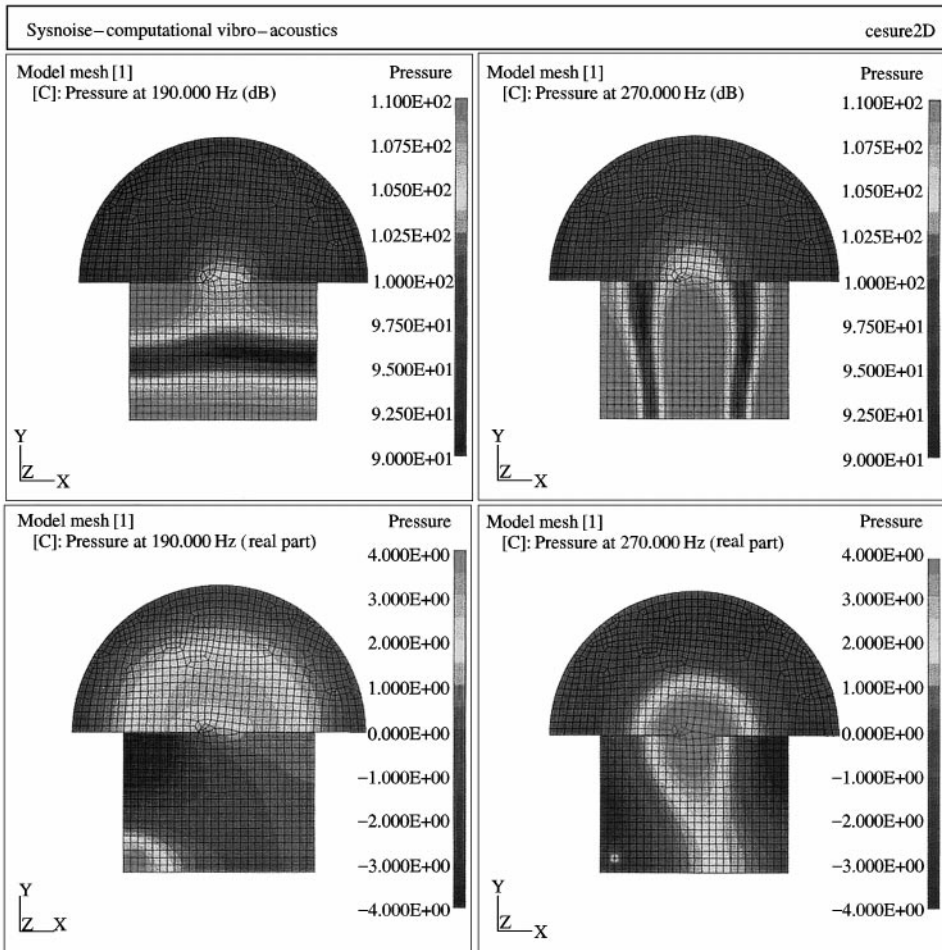


Figure 6. Section modes of the cavity — 2-D simulation.

3.2.2. Conclusion: a measurement of the noise radiated by the intercoach spacing

In addition to the analysis of the frequency content of the noise emitted by the ICS, the treatment of the sensors and probe signals provides an estimate of its noise level. The three sound spectra, indicative of the radiation of the whole cavity, computed from the signals of the three Noise probes, are superimposed in Figure 5. The intermediate Noise probe N2 delivers the highest level in the low-frequency range, whilst at high frequencies, the three spectra are similar and their levels decrease at the same rate. A first approximation of this level is given by the following formula:

$$\text{Spectrum (dB ref. } 2e^{-5} \text{ Pa)} = 80 - 35 (\log(f) - \log 300).$$

Finally, the root mean square (r.m.s.) values calculated for each spectrum are given in Table 1. They provide a global overview of the radiation of the inter-coach spacing.

TABLE 1
*Root mean square values of the noise radiated
 by the ICS at 350 km/h*

	N1	N2	N3
dB	117	118	113
dB (A)	99	103	97

4. RESPONSE TO THE FLOW AND RADIATION OF THE BOGIE

4.1. EXPERIMENTAL APPROACH AND INSTRUMENTATION

Twenty-one sensors were distributed around and under the bogie (see Figures 7 and 8) in order to characterize its acoustic behaviour. Four areas are distinguished:

1. *the area “above the bogie”*, characterized by the microphones P8, P9, P10, P13, P14, P24, P25, P26 and P27,
2. *the “outer middle” area*, approximately located under the cavity between the coaches and characterized by the microphones P7, P12, P13, P14, P18, P22, P23 and P24,
3. *the “outer left” area*, characterized by the microphones P12, P13, P18, P19, P20, P21, P22 and P25,
4. *the “outer right” area*, characterized by the microphones P7, P11, P15, P16, P17 and P23.

The spectra and coherence functions of these sensors have been analyzed to characterize the flow and to study its frequency distribution. Then, in order to determine whether the disturbance detected on the sensors radiate any sound or not, Noise probes are mounted outside the coaches at the level of the bogie in eight positions N_1 to N_8 (see Figure 7). They are distributed over the whole length of the bogie and are as close as possible to the estimated sources.

4.2. RESULTS AND ANALYSIS

4.2.1. *Characteristic frequencies*

The spectra given at 350 km/h by the sensors in area 3 are presented in Figure 9. This Figure indicates a strong disparity in the levels as well as in the frequency distribution of the detected signals.

The microphones giving the highest levels are those located in the incident flow, although nose cones protect some of them. Consequently, their signals are dominated by aerodynamical pressure fluctuations (turbulence). Furthermore, a peak at

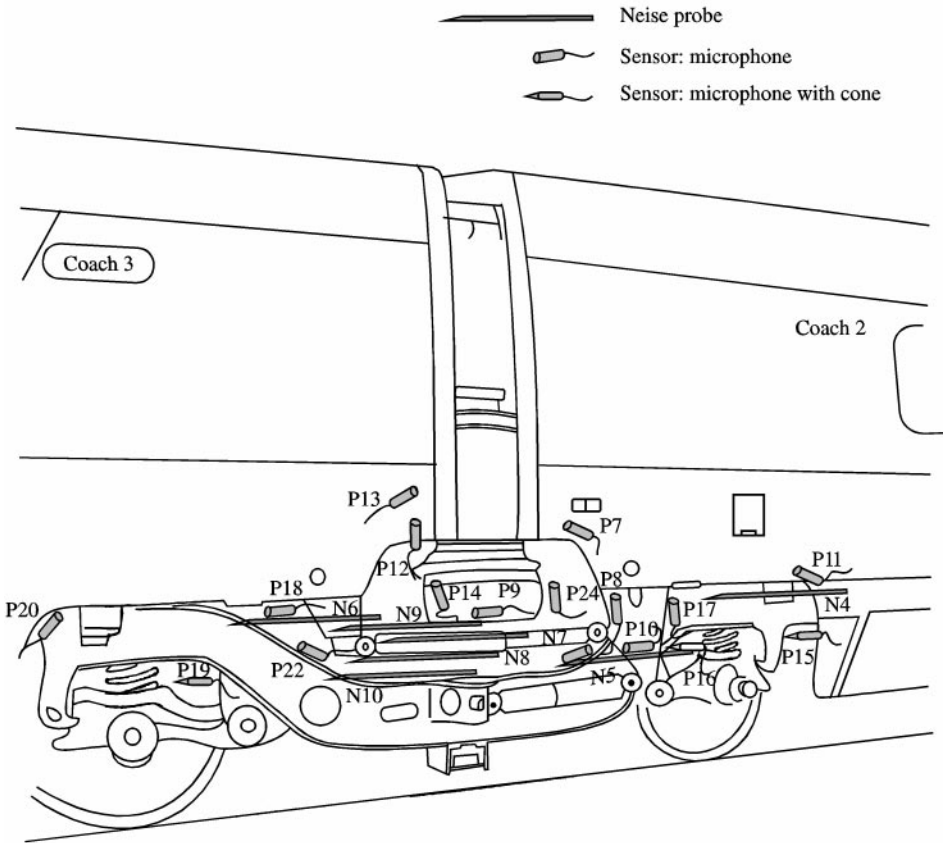


Figure 7. Location of the detection sensors in the bogie area (side-view).

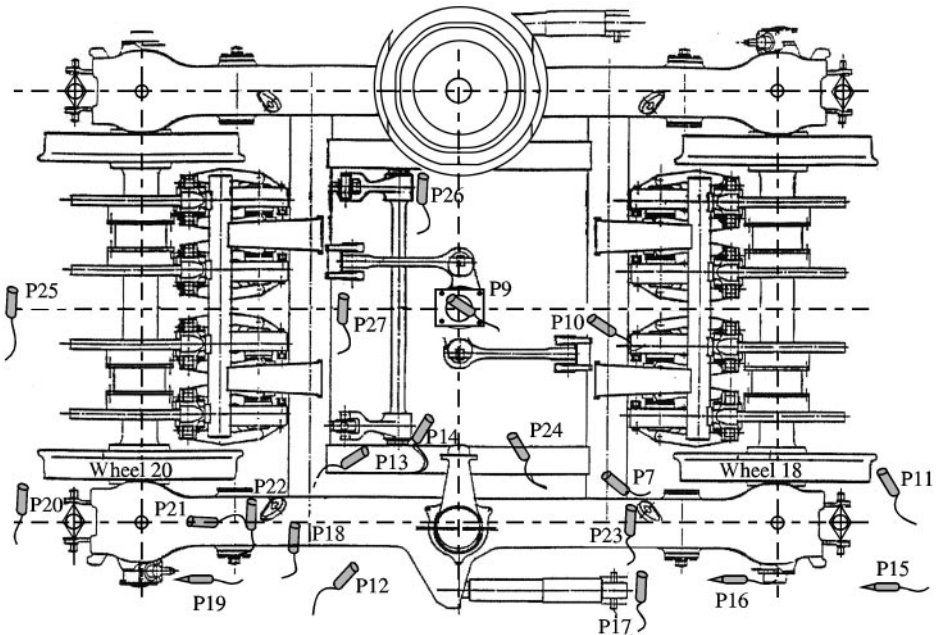


Figure 8. Location of the detection sensors and of the Neise probes in the bogie area (plain-view).

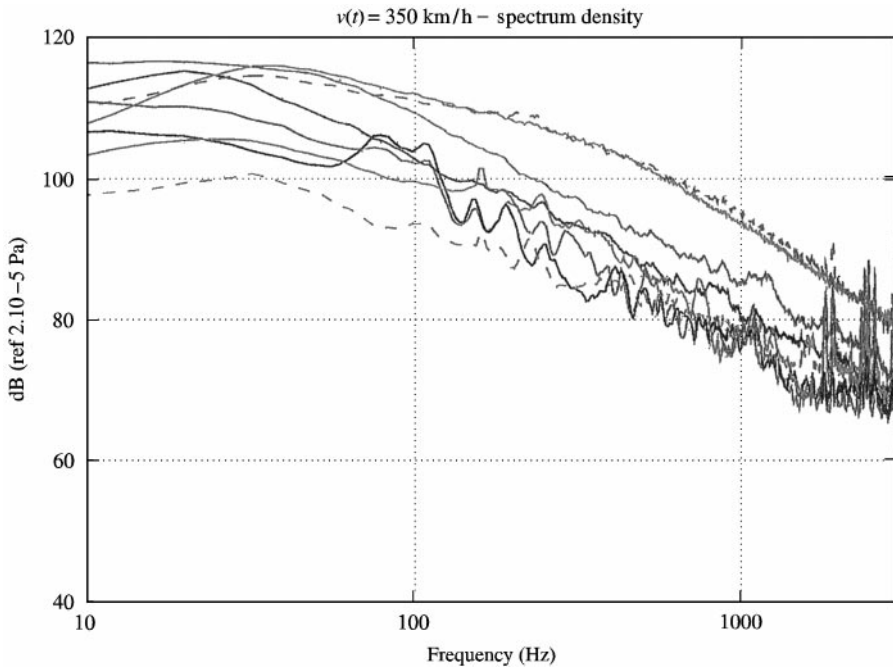


Figure 9. Spectra of the microphones located in the bogie area 3: “outer left area”. —, P12; —, P13; —, P18; —, P19; —, P20; - - , P21; —, P22; - - , P25.

about 164 Hz dominates the spectra. This frequency, which is the so-called sleeper-passing frequency, corresponds to the audible tone of the parametric excitation from the track at 350 km/h. Moreover, many peaks appear at high frequencies (around 2000 Hz and above). They are the main components of the rolling noise and correspond to the eigenmodes of the wheels that radiate under the excitation of the wheel/rail contact roughness.

In order to capture the frequencies of the disturbance induced by the flow around the bogie, the coherence functions between the sensors are computed. Then a selection of the most representative pairs of sensors in each zone and an averaging of the corresponding coherence functions allow efficient identification of the dominant frequencies. Table 2 lists these frequencies as well as the areas where they appear. A few frequency peaks (e.g., 252, 420, 520 and 680 Hz) appear in at least three distinct areas.

At this point, the dominance of only a few peaks can be noted, their frequencies listed and associated with one or several source areas. It is difficult to give further information about their physical mechanism or to specify whether they are linked to an acoustic source or not.

4.2.2. Radiated noise

The analysis of the spectra recorded with the Noise probes at 350 km/h leads to a selection of the most representative probes to study the radiation

TABLE 2

List of frequency peaks detected in bogie areas

Frequency (Hz)	Area 1	Area 2	Area 3	Area 4
76	X	X		
104		X		
116	X		X	
156		X		
164	X			X
196	X	X	X	X
204				X
121	X			
252	X	X	X	X
284		X		
312			X	
332				X
348	X	X		
380	X	X		
396			X	
420	X	X		X
440		X		X
476				X
492				X
520	X	X		X
552	X	X		
580				X
612				X
680	X	X		X
732	X	X		
796		X	X	
812				X
844				X
884			X	X
952				X
993			X	
1080			X	X

from each area:

- *the central areas*, above and outside the bogie (1 and 2): N8,
- *the left area* (3) (upstream): N6,
- *the right area* (4) (downstream): N4.

By plotting the coherence functions between these Noise probes and the detection probes of the corresponding area, the sensors which provide the most relevant coherence level can be selected. The highest coherence is found with the detection probes located outside the bogie; these are those most protected from the incident flow and which are the closest to the Noise probes.

This double selection is necessary to apply most efficiently the treatment method to estimate radiated noise, because of the great number of sensors and probes and possible comparative combinations. Finally, an efficient analysis of the radiation can be carried out with the microphones located in the external left and right areas:

- P20, P18 and P21 with N6 for the left area,
- P11 and P17, with N4 for the right area.

The spectra calculated with these detectors and in-flow probes are illustrated in Figures 10 and 11.

Left area: The spectrum shown in Figure 10 gives the sound level radiated by aeroacoustic sources located in the bogie area around the upstream wheel for nearly all frequencies between 10 and 1100 Hz. This spectrum clearly shows the following radiation phenomena:

- a noise peak at 196 Hz with a sound level around 85 dB,
- a pronounced peak at 252 Hz: its level fluctuates from 83 to 85 dB,
- a cluster of peaks between 300 and 400 Hz: their average level is about 77 dB,
- many peaks between 650 and 850 Hz, with an average level roughly equal to 72 dB,
- a very strongly pronounced peak at 1068 Hz, with a sound level of 75 dB.

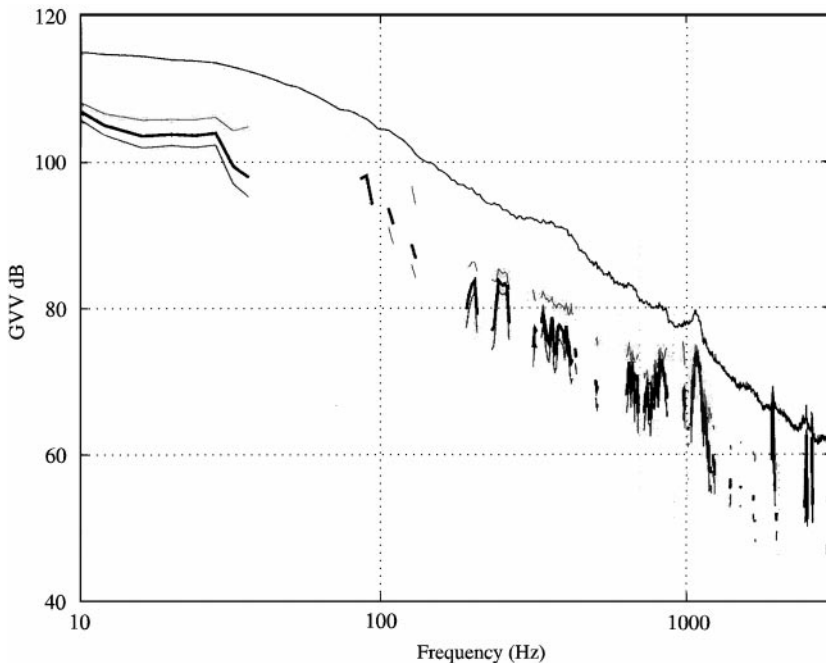


Figure 10. Estimation of the radiated noise with the direct method with the Noise probe N6a and the sensors P20a and P20b: (a) raw spectrum measured on the probe; (b) noise spectrum framed by its upper and lower margins of error. —, N6a measured; —, N6a corrected P20a-P20b; —, high error bar; —, low error bar.

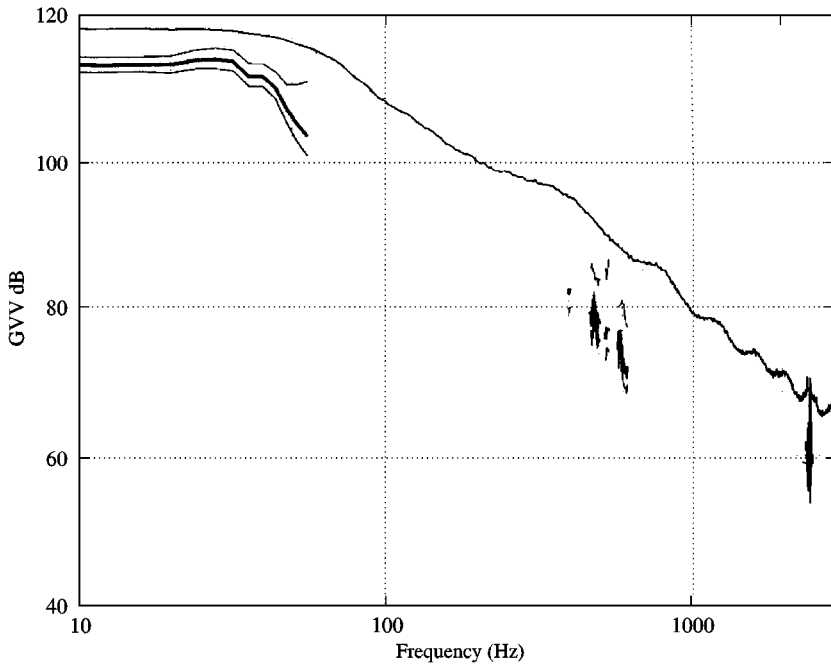


Figure 11. Estimation of the radiated noise with the direct method with the Noise probe N4 and the sensors P11 and P17: (a) raw spectrum measured on the probe; (b) noise spectrum framed by its upper and lower margins of error. —, N4 measured; —, N4 corrected P11–P17; —, high error bar; —, low error bar.

Right area: The spectrum shown in Figure 11 gives an estimate of the noise radiated by the outer area around the downstream wheel of the bogie. The estimate error restricts the noise curve to

- a broadband component between 0 and 50 Hz with a level of 115 dB,
- a few peaks at the following frequencies with the corresponding levels:
 - 476 Hz–80 dB,
 - 492 Hz–80 dB,
 - 580 Hz–75 dB,
 - 612 Hz–75 dB.

These frequencies were also detected in the bogie flow response. Thus, they are clearly characteristic of aeroacoustic radiation process.

Conclusion: Finally, different spectra are obtained which give a good and reliable value of the sound level for a few peaks and for some frequency bands between 0 and 1100 Hz. These bands correspond to the frequency range where aeroacoustic sources are predominant. In this analysis, noise peaks are detected at much higher frequencies than in the case of the ICS. Moreover, above 100 Hz, the acoustic average level decreases smoothly, with a slope of -35 dB per decade; this was also observed for the cavity.

Thus, a reliable evaluation of the acoustic contribution of a few local frequency phenomena was successfully carried out, although the methods presented and validated here have not been adapted to estimate the global level of noise radiated by the bogie. In particular, the sound pressure level at the point N6 radiated by the aeroacoustic sources located near the upstream wheel arch is characterized by an almost continuous spectrum and a 101 dB(A) r.m.s. value (120 dB r.m.s. value).

5. CONCLUSION

5.1. ABOUT THE MEASUREMENT METHOD

The following main objectives of the measurement method applied in the present study have been successfully achieved:

- localization of source regions,
- detection of particular sources,
- estimation of associated noise levels.

The results prove the efficiency and the reliability of the method. Source regions have been detected in the area around the bogie and in the ICS. For the latter, some have been physically identified. The associated levels are estimated together with an assessment of the accuracy of this estimation.

5.2. RADIATED NOISE

The measurements carried out in the ICS identify particular radiating phenomena at well-defined frequencies. Some phenomena are identified which are correlated with radiating modes of the ICS. An almost continuous acoustic spectrum is obtained; the noise emission is concentrated in the low-frequency range (below 500 Hz) and dominated by pure tones. Finally, the noise level radiated by the ICS, measured at a few centimetres from its opening, is estimated to be around 115 dB (linear) and 100 dB (A); consequently, it has a low impact on the global aerodynamic noise.

The results concerning the bogie area are generally more difficult to analyze than those obtained for the ICS since the coherent source mechanisms are unknown and appear to be more complex. Nevertheless, the treatment method yields some interesting and accurate results:

- No global aerodynamic mechanism describes the radiation from the whole bogie. It follows that the bogie cannot be modelled by a single source of noise but has to be considered as several uncorrelated acoustic sources.
- Many local coherent sources are detected under the bogie, but their contribution to the external radiation does not seem to be significant. However, other specific sources located in the up-stream and down-stream wheel arches radiate

efficiently, mainly in the frequency range 500–1000 Hz. Their contribution to the overall noise radiated by a TGV at 350 km/h is not negligible.

- The up-stream wheel arch radiates over a broad frequency range and its radiation is associated with an almost continuous spectrum extending to above 1000 Hz. Finally, the acoustic level of the noise radiated by this area, measured at the N6 position, is estimated to be about 120 dB (linear) and 101 dB (A).
- The acoustic spectrum associated with the downstream wheel arch also produces a few significant frequency peaks around 600 Hz.

ACKNOWLEDGMENTS

This study is part of the DEUFRAKO K2 project and was supported by the German and French Governments.

REFERENCES

1. J. S. BENDAT and A. G. PERSOL 1993 *Engineering Applications of Correlations and Spectral Analysis*. New York: John Wiley & Sons, Inc.
2. J. Y. CHUNG 1977 *Journal of Acoustical Society of America* **62**, 388–395. Rejection of flow noise using a coherence function method.
3. W. NEISE 1975 *Journal of Sound and Vibration* **39**, 371–400. Theoretical and experimental investigations of microphone probes for sound measurements in turbulent flows.